EFFECTS OF DRYING TEMPERATURES ON THE CRYSTALLITE SIZES OF METHYL AMMONIUM LEAD IODIDE PEROVSKITE ABSORBER LAYER

Hnin Yu Wai[1], Zin Min Tun[2] and Cho Cho Thet[3]

Abstract

In recent years, perovskite solar cells have attracted as a potentially inexpensive and high-performing materials for photovoltaic systems. The effects of drying temperature on the structural properties of methyl ammonium lead iodide ($CH_3NH_3PbI_3$) perovskite film, absorber layer in perovskite solar cell, was investigated in order to use on an electron transport layer (ETL) in perovskite solar cell. Perovskite film at different drying temperatures was prepared by two-steps spin coating method. Zinc stannate (Zn_2SnO_4) materials for electron collection layer was synthesized by chemical precipitation method. The optimum drying temperatures of $CH_3NH_3PbI_3$ perovskite absorber layer were varied by changing the drying temperatures at room temperature, 60, 100, and 150 ºC respectively. The crystal structures of final products of each layer were characterized by X-ray diffraction (XRD) technique. The surface morphology of $CH_3NH_3PbI_3/Zn_2SnO_4$/FTO films was observed by scanning electron microscope (SEM). The optimum drying temperature for perovskite absorber layer was found out to be 100 ºC for 30 min in air.

Keywords: perovskite, $CH_3NH_3PbI_3$, Zn_2SnO_4, spin coating, drying temperature, crystallite size

Introduction

Todays, environmental pollution is seriously causing due to the consumption of fossil energy globally. Thus, a great demand of renewable and sustainable energy sources is faced all over the world. The transformation of sunlight into electricity is considered one of the most hopeful researches to solve this situation without affecting the environment. Among the various kinds of solar cells, organic-inorganic hybrid perovskite solar cells (PSCs) have emerged as a potential candidate because of their high photovoltaic efficiency beyond 25% (Kheralla, A. and Chetty, N., 2021). Lead halide perovskites have great attention due to the development of simple thin-film deposition technology and low cost. They possess the outstanding photovoltaic performance including wide light harvesting in visible region, high absorption coefficients, low exciton binding energies, and long diffusion lengths high charge carrier mobility, and tunable direct bandgap (Dou, J., Zhang, Y., *et al*., 2019) and (Guo, R. *et al*., 2021). These properties lead to the candidates for the next generation of photovoltaic technology. The most commonly used perovskite absorber is methyl ammonium lead trihalide ($CH_3NH_3PbX_3$, where X is a halogen ion such as iodide, bromide, or chloride). It has an optical bandgap between ~1.55 and 2.3 eV, depending on halide content (Miah, M.H. *et al*., 2024).

The instability of PSCs is mainly depending on the environmental influences such as moisture, ultraviolet light, thermal, ion migration as well as the crystal structure, charge transporting layers (Wang, R. *et al*., 2019). It is remarkable that the crystal structure is influenced by the annealing temperature. The higher annealing temperatures and longer times can form the larger aggregated grains at the surface of the $MAPbI_3$ films (Rajendra Kumar, G. *et al*., 2016). To improve the photovoltaic performance, it is crucial to develop new materials for every layer of

[1] Department of Physics, East Yangon University
[2] Department of Physics, West Yangon University
[3] Department of Physics, University of Yangon

PSCs. They include the transparent conductive oxides layer, electron-transporting layers, perovskite absorber layers, hole-transporting layers and metal electrodes.

Among the key component in PSCs, the ETLs is largely affect for interfacial carrier extraction and electron transporting, which are significantly relevant to photovoltaic performance (Liu, X. *et al*., 2022).

For electron transporting layer of PSCs, stannate family has been greatly interested in the last decade because its photocatalytic properties such as high electrical conductivity and low visible absorption. The spinel type zinc stannate Zn_2SnO_4 is one of the important members of stannate family. It is a n-type semiconductor which has wide band gap of 3.6 eV and electron mobility of 10^{-15} cm^2 V^{-1} s^{-1} (Dou, J., Shen, D., *et al*., 2019). Because of its properties, it can be applied in many fields of applications such as gas sensor, synergistic flame retardants, solar cells, luminescence materials, anode electrode for Li-ion batteries, and degradation of organic pollutants (Mekprasart, W. *et al*., 2016). In this work, the effect of annealing temperature on the perovskite layer which is spin-coated on the electron transport layer of Zn_2SnO_4/FTO will be investigated.

Experimental Details

Preparation of Zn_2SnO_4/ FTO Film

Zn_2SnO_4 particles was synthesized by chemical precipitation method. Zinc sulfate heptahydrate ($ZnSO_4.7H_2O$) and tin (IV) chloride pentahydrate ($SnCl_4.5H_2O$) are used as the starting materials. Sodium hydroxide (NaOH) and distilled water (DW) are used as the precipitating agent and a solvent. Firstly, 2 M of $ZnSO_4.7H_2O$ solution and 1 M of $SnCl_4.5H_2O$ solution were separately prepared by DW. In addition, the zinc sulfate solution was sonicated for 30 min in order to get a homogeneous solution. Later, the two solutions were mixed and stirred for 30 min at room temperature. Then, pH of the solution was adjusted by using 1 M of NaOH until to become the pH 9.5. The solution was stirred for 6 h at 70 ºC and aged for 16 h. The white precipitates were rinsed with DW for several times until the pH of the solution became neutral. Finally, the precipitates were dried at 80 ˚C and they were grinded by agate mortar and pestle. The fine powder was calcined at 1000 ºC for 1 h. Finally, Zn_2SnO_4 particles were successfully obtained.

For the film formation, fluorine doped tin oxide coated *glass* (FTO) is used as a substrate. FTO substrate was cleaned by ultrasonic cleaning in ethanol, acetone and distilled water for 30 min in each solvent respectively. The Zn_2SnO_4/FTO film is prepared by spin coating method. 1 g of Zn_2SnO_4 is dissolved in 4 mL of mixed solvent containing IPA and ethanol (volume 1:1 %). The solution was stirred continuously for several days and Zn_2SnO_4 solution was obtained. 50 μL of Zn_2SnO_4 solution was spin coated onto the 1×1 cm^2 of FTO at 3000 rpm for 60 s. Then, Zn_2SnO_4/FTO film was dried at 100 ºC for 30 min inside the muffle furnace. The preparation procedure of Zn_2SnO_4/ FTO film is expressed in Figure 1.

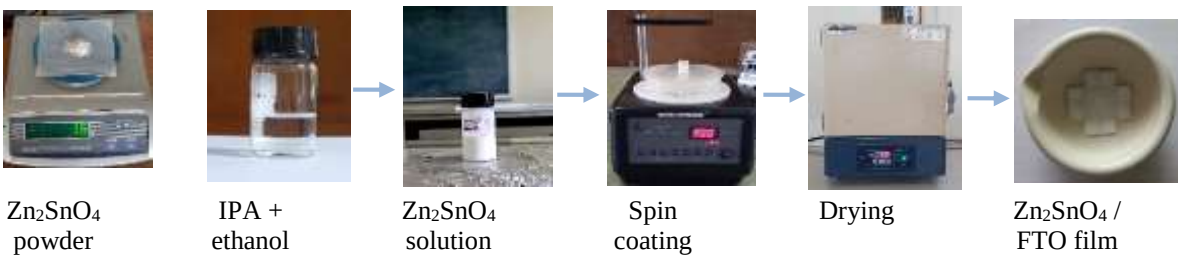

Figure 1. Photograph of the preparation of Zn_2SnO_4/ FTO film

Preparation of Perovskite Absorber Layer

Perovskite absorber layer ($CH_3NH_3PbI_3$) is prepared by two-steps spin coating method. In the first step, 2.305 g of PbI_2 powder was mixed with 5 mL of mixed solution containing dimethylformamide (DMF) and dimethyl sulfoxide (DMSO). The DMF to DMSO was volume 9:1 %. Then, PbI_2 solution was stirred at 60 ºC for 2 h and the well dissolved solution was filtered by filter paper. The clear PbI_2 filtrate was obtained. The thin PbI_2 film was spin-coated from a clear 50 μL of PbI_2 solution at 3,000 rpm for 30 s and 1500 rpm for another 30 s on **Zn_2SnO_4/FTO layer** in order to form the PbI_2/**Zn_2SnO_4/FTO layer**.

For the second step, CH_3NH_3I (MAI) solution was prepared by adding 0.0159 g of MAI into 1 mL of 2-propanol and it was stirred for 2 h. After that, 50 μL of MAI solution was spin-coated onto the previous layer to form $CH_3NH_3PbI_3$ perovskite films. Then, the films were dried at room temperature (RT), 60, 100 and 150 ºC in the muffle furnace for 30 min respectively. Finally, **$CH_3NH_3PbI_3$/Zn_2SnO_4/FTO film was successfully obtained.** The varying of drying temperature is carried out in order to investigate the crystallinity and crystallite size of perovskite layer for the further step in the fabrication of solar cell.

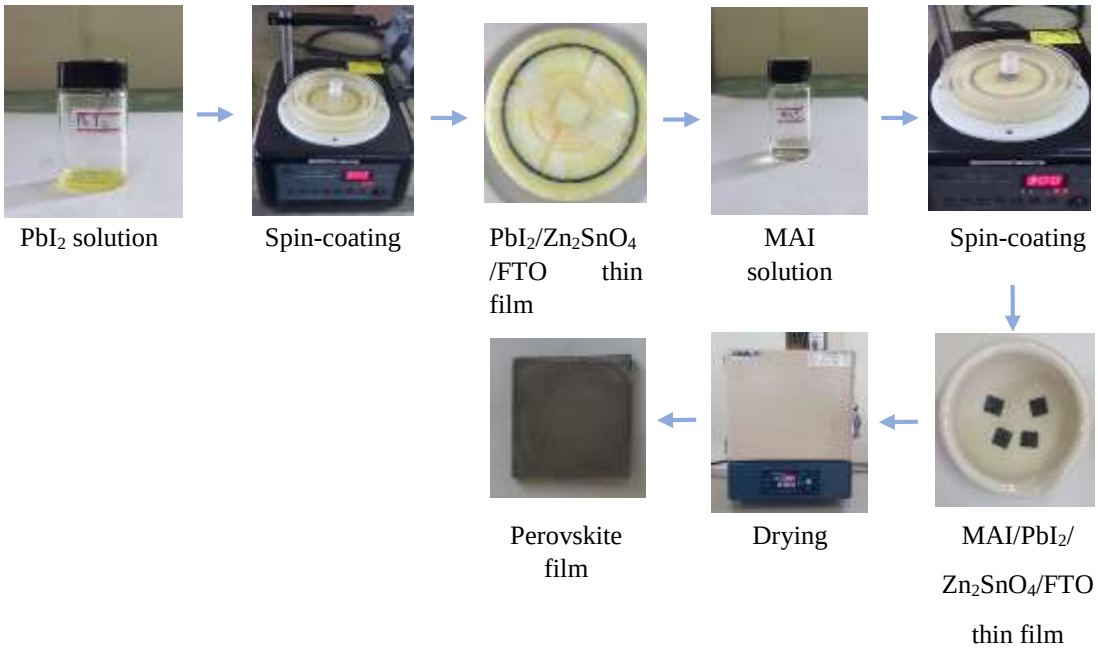

Figure 2 Photograph of the preparation of $CH_3NH_3PbI_3/Zn_2SnO_4$/FTO film

Results and Discussion

In this work, XRD measurements are carried out to confirm the electron collection layer (zinc stannate) and perovskite absorber layer ($CH_3NH_3PbI_3$). XRD spectra of Zn_2SnO_4 powder calcined at 1000 ºC for 1 h are shown in Figure 3(a). The X-ray diffraction peaks for (111), (220), (311), (222), (400), (331), (422), (511), (440), (531), (442), (620), (533), (622), (444) and (711) planes were confirmed that the formation of *inverse spinel structure* of Zn_2SnO_4 with *stable phase.* These Miller indices indicated that the zinc stannate is cubic crystal structure.

As indicated in Figure 3(b), the peak observed at the 14.01° was corresponded to the first reflection of the perovskite phase. All the remaining peaks were also related to $CH_3NH_3PbI_3$. The crystal structure of perovskite absorber layer was found out to be orthorhombic structure. The

average crystallite size of Zn_2SnO_4 and perovskite was calculated by the Debye-Scherrer Equation as below.

$$D = \frac{K\lambda}{\beta \cos\theta} \quad (1)$$

where,

λ = wavelength of the incident X-ray beam
K = shape factor
β = width at half maximum (FWHM)
θ = diffraction angle
D = crystallite size

The average crystallite size of Zn_2SnO_4 was obtained 66.50 nm. Table 1 is listed for the $CH_3NH_3PbI_3/Zn_2SnO_4$/FTO at different drying temperatures. The crystallite size was the smallest for the film dried at 100 ºC since most of the OH groups were removed at this temperature and thus the crystallite is the reduced. As a result, the biggest size is obtained at the lowest drying temperature. However, when the temperature was increased to 150 ºC, the size was tended to increase again due to thermal expansion (Zamkovskaya, A. *et al*. 2017).

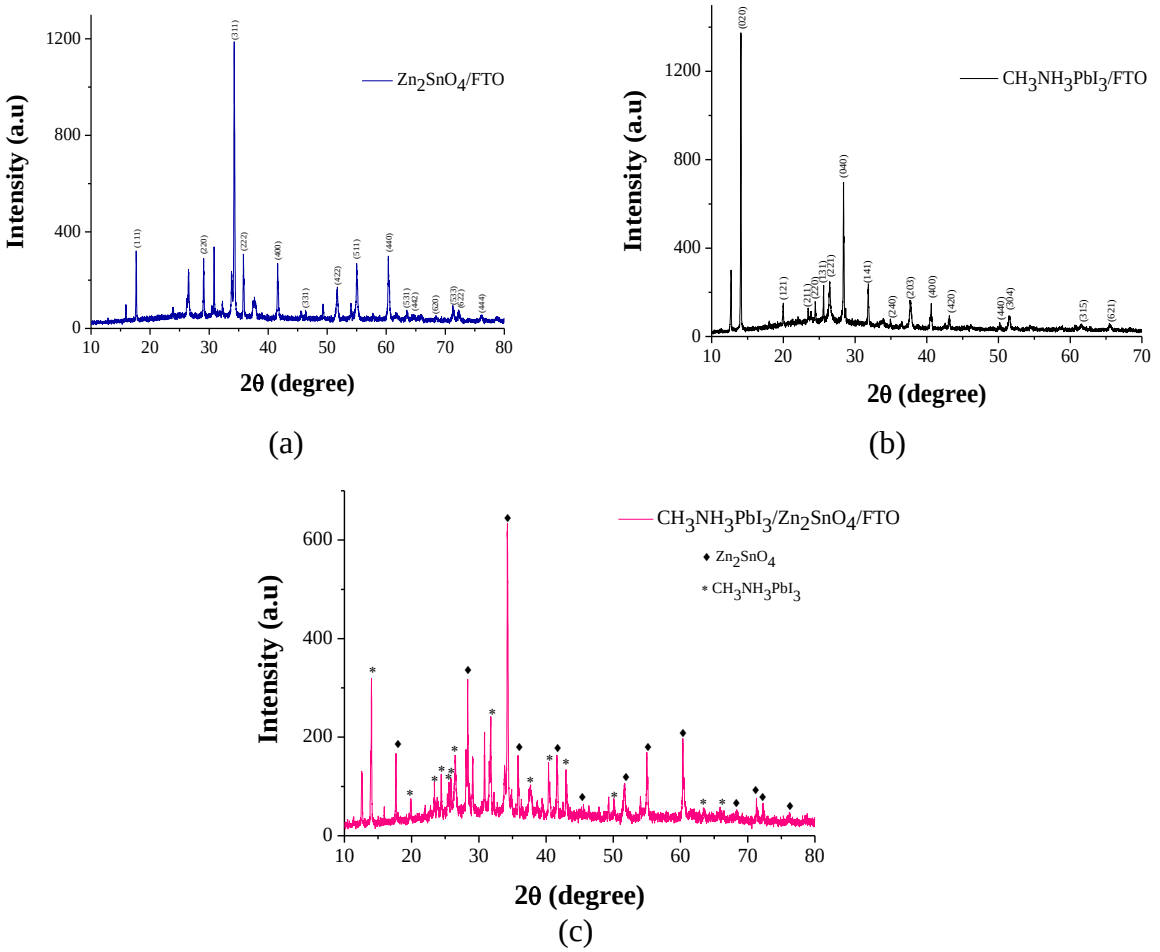

Figure 3 XRD spectrum of (a) Zn_2SnO_4/FTO film, (b) $CH_3NH_3PbI_3$/FTO film and (c) $CH_3NH_3PbI_3/Zn_2SnO_4$/FTO film

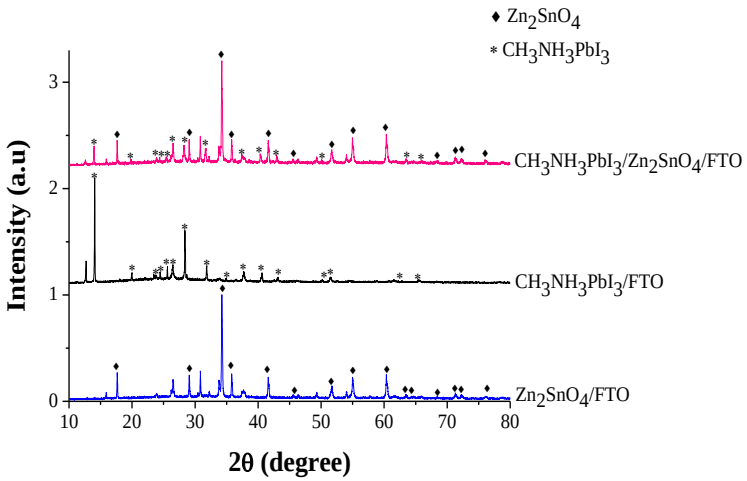

Figure 4 XRD spectra of different layers on FTO substrate

The typical XRD pattern of thin film dried at different temperatures are exhibited in Figure 5. The symbols * indicated the peaks from $CH_3NH_3PbI_3$. All the remaining peaks were corresponded to Zn_2SnO_4. In all temperatures, all perovskite peaks were found at 14.01°. However, the most intense peak of perovskite was occurred at 100 ºC among the different temperatures.

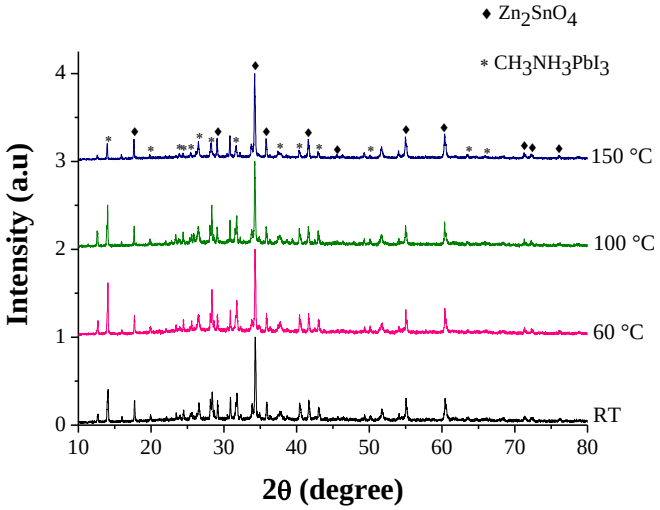

Figure 4 XRD spectra CH3NH3PbI3/ Zn2SnO4/ FTO film

Table 1. XRD parameters of $CH_3NH_3PbI_3$/ Zn_2SnO_4/ FTO film

Drying temperature (ºC)	Lattice parameters (Å)			Average crystallite size (nm)
	a	b	c	
RT	8.91	12.69	8.73	68.3
60	8.92	12.69	8.52	46.7
100	8.82	12.66	8.56	24.9
150	8.94	12.75	8.68	66.8

SEM measurement is conducted in order to study each layer formation in the film. The SEM micrograph in Figure 6 shows the cross-section of $CH_3NH_3PbI_3/Zn_2SnO_4$/FTO film. Glass, FTO, Zn_2SnO_4 and $CH_3NH_3PbI_3$ layers were distinctly observed in the image. This image supports the formation of each spin-coated layer that were previously presented in the XRD results.

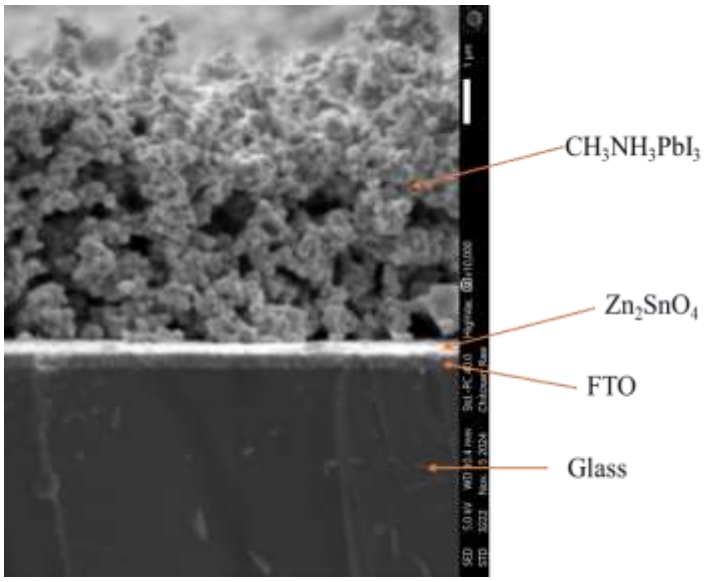

Figure 6 Cross-section SEM image of $CH_3NH_3PbI_3/Zn_2SnO_4$/FTO film

Conclusions

Methyl ammonium lead iodide ($CH_3NH_3PbI_3$), perovskite absorber layer, on zinc stannate (Zn_2SnO_4) was successfully prepared by two-steps spin coating method. Zn_2SnO_4 was synthesized by chemical precipitation method. According to XRD results, the crystal structure of Zn_2SnO_4 and $CH_3NH_3PbI_3$ were cubic and orthorhombic respectively. The crystallite sizes estimated by Debye-Scherrer formula was occurred 66.5 nm for Zn_2SnO_4 and 68.3, 46.7, 24.9 and 66.8 nm respectively for $CH_3NH_3PbI_3$ at RT, 60, 100 and 150 ºC. The sharpest peak for finger print of perovskite and the smallest crystallite sizes were observed at 100 ºC. Although the crystallite depending on drying temperatures were changed, they have the crystal structures. Thus, it can be concluded that 100 ºC is the optimum the drying temperature for the formation of perovskite layer.

Acknowledgements

We would like to acknowledge to Prof Dr Nay Win Oo, Rector, East Yangon University, for his encouragement and allowing us to participate in this event. Our special thanks go to Dr Hmwe Hmwe Kyu, Professor and Head of Department of Physics, East Yangon University, for her kind permission to contribute this work excellent discussion.

References

Dou, J., Shen, D., et al. (2019) 'Highly Efficient Perovskite Solar Cells Based on a Zn2SnO4 Compact Layer', ACS Applied Materials and Interfaces, 11(40), pp. 36553–36559. Available at: https://doi.org/10.1021/acsami.9b09209.

Dou, J., Zhang, Y., et al. (2019) 'Highly efficient Zn2SnO4 perovskite solar cells through band alignment engineering', Chemical Communications, 55(97), pp. 14673–14676. Available at: https://doi.org/10.1039/c9cc07398a.

Guo, R. et al. (2021) 'Ambient processed (110) preferred MAPbI3thin films for highly efficient perovskite solar cells', Nanoscale Advances, 3(7), pp. 2056–2064. Available at: https://doi.org/10.1039/d0na01029d.

Kheralla, A. and Chetty, N. (2021) 'A review of experimental and computational attempts to remedy stability issues of perovskite solar cells', Heliyon, 7(2), p. e06211. Available at: https://doi.org/10.1016/j.heliyon.2021.e06211.

Liu, X. et al. (2022) 'Area-Scalable Zn2SnO4Electron Transport Layer for Highly Efficient and Stable Perovskite Solar Modules', ACS Applied Materials and Interfaces, 14(20), pp. 23297–23306. Available at: https://doi.org/10.1021/acsami.1c24757.

Mekprasart, W. et al. (2016) 'Synthesis and characterization of cubic-like zinc stannate powders prepared by co-precipitation method', Chiang Mai Journal of Science, 43(2), pp. 345–350.

Miah, M.H. et al. (2024) 'Band gap tuning of perovskite solar cells for enhancing the efficiency and stability: issues and prospects', RSC Advances, 14(23), pp. 15876–15906. Available at: https://doi.org/10.1039/d4ra01640h.

Rajendra Kumar, G. et al. (2016) 'Phase transition kinetics and surface binding states of methylammonium lead iodide perovskite', Physical Chemistry Chemical Physics, 18(10), pp. 7284–7292. Available at: https://doi.org/10.1039/c5cp06232b.

Wang, R. et al. (2019) 'A Review of Perovskites Solar Cell Stability', Advanced Functional Materials, 29(47), pp. 1–25. Available at: https://doi.org/10.1002/adfm.201808843.

Zamkovskaya, A. et al. (2017) 'X-ray diffraction investigations of the thermal expansion of iron borate FeBO3 crystals', Journal of Physics: Conference Series, 929(1). Available at: https://doi.org/10.1088/1742-6596/929/1/012030.